EMU Notes in Mineralogy, Vol. 16 (2017), Chapter 11, 347–371

Nucleation in geological materials

FRED GAIDIES

Department of Earth Sciences, Carleton University, 1125 Colonel By Drive, Ottawa, Ontario, K1S 5B6, Canada, e-mail: Fred.Gaidies@carleton.ca

Nucleation is the initial process of most phase transformations and is of fundamental importance for the kinetics of mineral reactions. A departure from equilibrium is required to overcome the energy barrier associated with nucleation, which is a function of the structural and compositional differences between the nucleus and the metastable reactant, and the level of elastic deformation experienced by the nucleus as it forms in the host lattice. Nucleation in geological materials almost always takes place at grain boundaries, crystal defects or impurities, which catalyse the nucleation process and influence the chemical composition, size, shape, lattice orientation and spatial distribution of nuclei with important implications for the texture and microstructure evolution of rocks. Nuclei are microscopic in most systems and thus are too small to be observed in experiment. This is why nucleation has been intensively studied theoretically and through numerical simulations. In those treatments, nucleation integrates more elementary processes such as chemical diffusion and interface motion.

This chapter provides the essential physics of the thermodynamics and kinetics of nucleation. It reviews the fundamentals of the classical nucleation theory including the chemical driving force for nucleation in partitioning systems and the interfacial area of clusters, discusses possible nucleus/substrate interactions and their influence on the free energy of the nucleus and the energy barrier to nucleation, and presents expressions for the classical nucleation rate. In a second part, extensions to CNT are outlined that couple long-range diffusion with the kinetics of interface processes in order to address the formation of nucleation exclusion or depleted zones around supercritical clusters and the enrichment of the precipitated components in the vicinity of subcritical clusters. Finally, the reader is introduced to non-classical gradient-energy continuum approaches to nucleation in inhomogeneous systems, and to the phase field method for the simulation of microstructure evolution.

1. Classical nucleation theory

Classical nucleation theory (CNT) is a model developed to quantify and predict the initial process during phase transformations associated with an energy barrier caused by structural differences between a reacting and product system. This type of phase transformation is referred to as discontinuous phase transformation. In its initial form, CNT is based on the work of Gibbs (1928) who introduced the concept of interfaces of zero thickness between homogenous phases in his attempt to develop a formulation for the thermodynamics of heterogeneous systems. Kaischew and Stranski (1934) extended CNT in their application to the formation of crystals from supersaturated vapour, based on work done previously by Volmer and Weber (1926) on vapour

DOI: 10.1180/EMU-notes.16.11

condensation. Contributions by Becker and Döring (1935), Volmer (1939), Frenkel (1946), and Turnbull and Fisher (1949) expanded CNT for application to condensed systems. CNT may now be the best known quantitative approach to nucleation as it successfully predicts the main features of nucleation in appropriate systems irrespective of its inherent approximations.

At the heart of CNT is the description of the energy barrier associated with the formation of the interface between reactants and products of a discontinuous phase transformation, and a formalism that links this energy barrier to the kinetics of molecular attachment and detachment processes at the interface. Because long-range diffusion through the reacting system is not accounted for, CNT is an inherently interface-limited model.

1.1. Energy barrier to nucleation

The nucleation barrier is assumed to be a function of the energy required to form the structural transition across the product-reactant interface per unit interfacial area, σ, and the chemical force that drives nucleation, ΔG_V. For a given pressure (P), temperature (T) and bulk chemical composition (X), ΔG_V is the difference in bulk Gibbs energy between reacting system and nucleating phase, per product molecule. For an interfacial area that is composed of i individual regions, A_i, the Gibbs energy of formation of a product cluster with n molecules, ΔG_n, is written

$$\Delta G_n = n\Delta G_V + \sum_i A_i\sigma_i \tag{1}$$

Because ΔG_V is negative in a thermodynamically favoured phase transformation and $\Sigma\sigma_i$ is always positive, and because the contribution of the interfacial energy term to ΔG_n is larger than that of the bulk term for relatively small n given the surface to volume relationship, ΔG_n develops a maximum before it decreases and becomes negative with an increase of cluster size.

If σ is direction-independent, a spherical cluster geometry can be assumed so that equation 1 simplifies to

$$\Delta G_n = n\Delta G_V + (36\pi)^{1/3}(\bar{v}n)^{2/3}\sigma \tag{2}$$

where $\bar{v}$ is the volume of a molecule in the cluster. Figure 1 illustrates the relationship between ΔG_n and n assuming a spherical cluster geometry.

In general, clusters with a size that maximizes ΔG_n are referred to as nuclei (or critical clusters), and their formation is called nucleation. The number of molecules contained in a spherical critical cluster, n^*, can be found by differentiation of (2) and is given by

$$n^* = \frac{-32\pi\bar{v}^2\sigma^3}{3(\Delta G_V)^3} \tag{3}$$

so that its radius, r^*, is equal to

$$r^* = \frac{-2\bar{v}^2\sigma}{\Delta G_V} \tag{4}$$

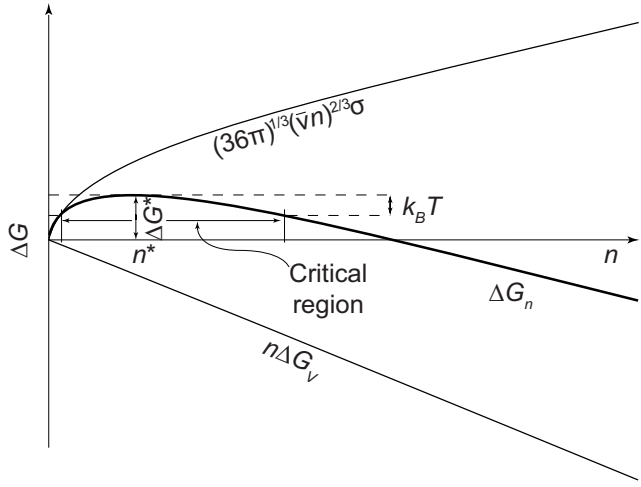

Figure 1. The Gibbs energy of cluster formation, ΔG_n, as a function of the number of molecules per product cluster, n, assuming an isotropic interfacial energy, σ, and a negative chemical driving force for nucleation, ΔG_V. ΔG^* is the critical energy barrier to nucleation, and n^* refers to the number of molecules in the critical cluster.

The maximum of ΔG_n (Fig. 1) can be obtained by combining equations 2 and 3, and is given by

$$\Delta G^* = \frac{16\pi\bar{v}\sigma^3}{3(\Delta G_V)^2} \tag{5}$$

ΔG^* represents the energy barrier which has to be overcome to form critical clusters of the product of the discontinuous phase transformation. These clusters are in unstable equilibrium with the reacting system because the decomposition of subcritical clusters ($n < n^*$) and the attachment of additional molecules to the surfaces of supercritical clusters ($n > n^*$) are energetically favoured as that decreases ΔG_n (Fig. 1). Cluster sizes for which

$$\Delta G^* \geqslant \Delta G_n \geqslant \Delta G^* - k_B T \tag{6}$$

where k_B is Boltzmann's constant, mark the critical region of nucleation (Fig. 1). According to equations 3 and 5, the critical cluster region as well as n^* and ΔG^* increase with a decrease in ΔG_V so that discontinuous phase transformations close to equilibrium require relatively fast transfer processes at the interface for nucleation to take place. Note that CNT does not define n^* and ΔG^* for $\Delta G_V = 0$. An increase in ΔG_V results in a decreasing energy barrier to nucleation and smaller critical clusters as fewer molecules are required for their formation. In the case of exceedingly small critical clusters, the separation of bulk and interfacial energy terms, expressed in equation 1 and referred to as capillarity approximation of CNT, cannot be applied and alternative methods such as the Cahn-Hilliard approach (section 3) may be used.

1.1.1. Chemical driving force and nucleus composition in partitioning systems

The chemical driving force for nucleation, ΔG_V, is the Gibbs energy change associated with the formation of a small amount of the product phase out of the metastable reacting system, per molecule of the new phase. It may be seen as the Gibbs energy per product molecule that drives the processes underlying nucleation such as molecular attachment and detachment processes at the interface and migration of the interface into the reactant. In a partitionless discontinuous phase transformation, the nucleus grows with the same composition as the reactant. However, nucleation in natural systems is commonly a partitioning process so that the composition of the nucleus differs from that of the reacting system. In such a case, the Gibbs energy change is maximized if the differences in chemical potentials between metastable reacting system and nucleus of the components involved in the phase transformation are identical.

For a binary system with components A and B the composition of the nucleus, x^P_{nuc}, can be determined graphically by the point of tangency on the G–x function of the product, P, of a line that is parallel to the tangent that corresponds to the energy state of the reactant, R (stippled lines in Fig. 2c,d). As shown in Fig. 2c, x^P_{nuc} in partitioning systems differs from the equilibrium composition of the product, x^P_{equ}. The difference

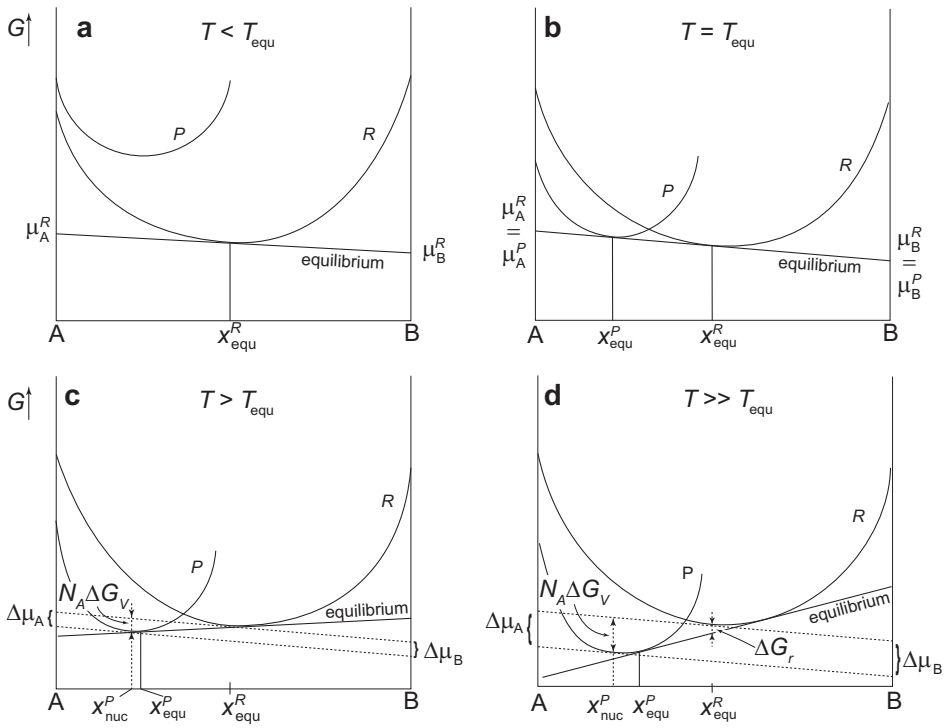

Figure 2. Schematic molar Gibbs energy diagrams for the binary system A–B illustrating the relationship between ΔG_V, ΔG_r, X^P_{nuc}, X^P_{equ}, X^R_{equ} and the departure from equilibrium. N_A is Avogadro's constant.

between x^P_{nuc} and x^P_{equ} increases with departure from equilibrium required to overcome the energy barrier to nucleation, and depends on the $G{-}x$ relationships of the phases involved (Fig. 2d), provided that the bulk composition of the system, x^R_{equ}, does not change during the nucleation. Once nucleated, the product will change its composition towards equilibrium with the surrounding reactant if diffusion within the product and reacting system and across their interface is efficient. The molar Gibbs energy difference between the initial and final equilibrium states, ΔG_r (Fig. 2d), is the maximum available force that drives all the processes of the overall phase transformation. Diffusion transfers material between *R* and *P* resulting in the growth of *P* and the dissipation of Gibbs energy until equilibrium is established. This may be visualized by rotating the two stippled parallel lines in Fig. 2 tangential to *R* and *P* until they coincide with the single equilibrium tangent to *R* and *P* (equilibrium line in Fig. 2c, d). ΔG_r may be obtained through integration over the Gibbs energy dissipated during the diffusion. The total amount of ΔG_r that can be dissipated depends on the bulk composition of the system, x^R_{equ}, and reaches a maximum if x^R_{equ} approaches x^P_{equ}.

The tangent-method may also be applied to nucleation in multicomponent systems and was utilized by Gaidies *et al.* (2011) to estimate ΔG_V associated with the contact metamorphic nucleation of garnet in a metapelite of the aureole of the Nelson Batholith (British Columbia, Canada). The reacting rock matrix was modelled as a $MnO–Na_2O–CaO–K_2O–FeO–MgO–Al_2O_3–SiO_2–H_2O–TiO_2$ (MnNCKFMASHT) system using the thermodynamic data of Holland and Powell (1998). The matrix was assumed to be equilibrated at any point in *P-T* space, but the nucleation of garnet was assumed to be kinetically hindered. Such a scenario may be envisioned for the nucleation of phases with structural properties significantly different from those of the phases in the reacting system, and where diffusion in the reacting system is faster than across the interface with the nucleus. ΔG_V is calculated based on the tangent-method outlined above and is illustrated in Fig. 3a as a function of the departure from equilibrium.

Note that the coloured *P-T* regions correspond to the conditions where ΔG_V is negative so that the formation of garnet is thermodynamically favoured. In general, ΔG_V increases with thermal overstep of the low-*T* conditions of the stability field of garnet-bearing assemblages, and decreases towards the high-*T* limit. Similar to the exemplarily binary system, ΔG_V associated with the crystallization of garnet in multicomponent systems is a function of the $G{-}x$ relationships of the matrix phases and garnet, and how these thermodynamic properties vary with temperature and pressure. The lower *T* limits at which staurolite and andalusite enter the matrix assemblages are characterized by a "channel" in ΔG_V-*P-T* space and mark the conditions with the highest garnet nucleation probability (stippled line in Fig. 3a).

Figure 3b shows ΔG_r associated with the formation of garnet from the respective phase assemblages in the modelled bulk chemical system. It can be seen that ΔG_r differs from ΔG_V not only quantitatively but also with respect to its dependence on *P-T*. Whereas ΔG_V reflects the force on a product molecule involved in the formation of a critical cluster, ΔG_r corresponds to the integrative molar Gibbs energy that dissipates through the entire transformation process. Hence, ΔG_V can be understood as part of ΔG_r, but because relatively few molecules are involved in nucleation compared to the

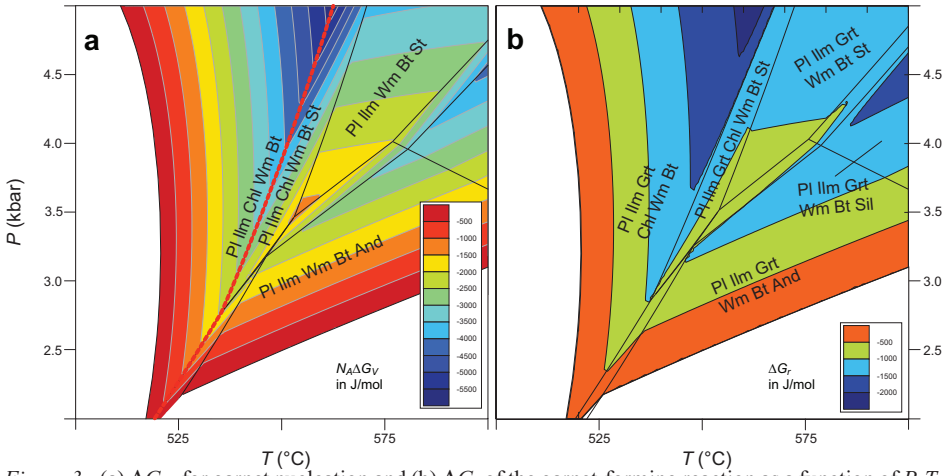

Figure 3. (a) ΔG_V, for garnet nucleation and (b) ΔG_r of the garnet-forming reaction as a function of *P-T*. Modified after Gaidies *et al.* (2011). And – andalusite, Bt – biotite, Chl – chlorite, Grt – garnet, Ilm – ilmenite, Pl – plagioclase, Sil – sillimanite, St – staurolite, Wm – white mica.

growth of the particles to macroscopic crystal sizes, the majority of ΔG_r is used for the diffusion associated with crystal growth.

Similar to ΔG_V, the differences between x^P_{nuc} and x^P_{equ} of garnet increase with departure from equilibrium. Whereas the differences between x^P_{nuc} and x^P_{equ} are small with respect to the pyrope and grossular contents of garnet, the spessartine and almandine contents of a nucleus differ significantly from the equilibrium composition (Fig. 4). Even though chemical fractionation during garnet crystallization is common, reflecting relatively low rates of diffusion in garnet, and irrespective of its influence on the thermodynamically effective bulk composition, the impact of chemical fractionation on ΔG_r, ΔG_V and garnet chemistry cannot be shown in a *P-T* diagram because it is dependent on the *P-T* path of crystallization.

1.1.2. Elastic strain energy

If there are differences in the volume or shape between the nucleating phase and the reacting host then the energetics of nucleation may involve elastic strain energy, ΔG_E. This instance may be particularly relevant for discontinuous phase transformations at the solid state. In the case of lattice misfits, ΔG_E will be positive and will scale with the volume of the nucleus so that equation 1 changes to

$$\Delta G_n = n(\Delta G_V + \Delta_E) + \sum_i A_i \sigma_i \tag{7}$$

Assuming a spherical nucleus geometry and an isotropic interfacial energy, ΔG_n can be written as

$$\Delta G_n = \frac{4\pi r^3}{3\bar{v}} (\Delta G_V + \Delta G_E) + 4\pi r^2 \sigma \tag{8}$$

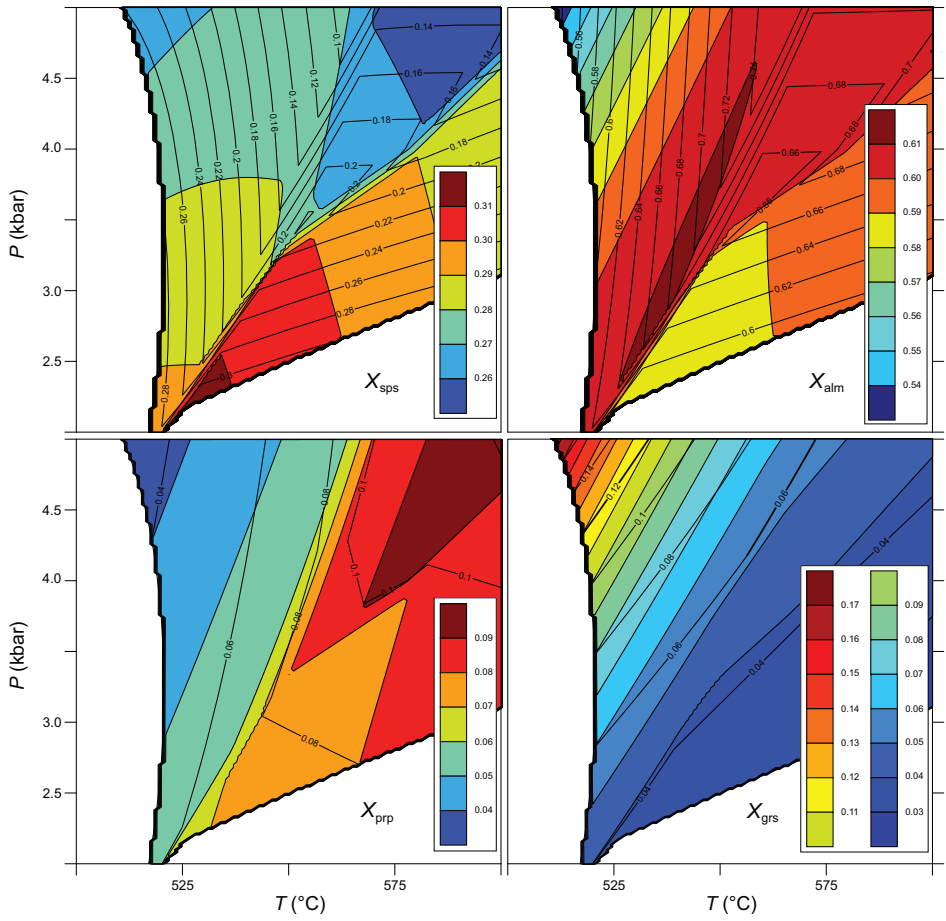

Figure 4. Equilibrium composition of garnet (isopleths) as a function of *P*-*T*, and chemical composition of a garnet nucleus (coloured) for different degrees of overstepping. After Gaidies *et al.* (2011). X_{sps} = Mn/(Fe^{2+}+Ca+Mg+Mn), X_{alm} = Fe^{2+}/(Fe^{2+}+Ca+Mg+Mn), X_{prp} = Mg/(Fe^{2+}+Ca+Mg+Mn), and X_{grs} = Ca/(Fe^{2+}+Ca+Mg+Mn).

where the volume of a cluster corresponds to $n\bar{v}$. Hence, r^* can be written as

$$r^* = \frac{-2\bar{v}\sigma}{\Delta G_V + \Delta G_E} \tag{9}$$

so that

$$\Delta G^* = \frac{16\pi\bar{v}^2\sigma^3}{3(\Delta G_V + \Delta G_E)^2} \tag{10}$$

According to equation 8, nucleation can only take place if $\Delta G_E < |\Delta G_V|$. Hence, the interfacial term and ΔG_E of equation 10 represent the energy penalty to nucleation as they both increase ΔG^* in a thermodynamically favoured phase transformation.

In general, ΔG_E is proportional to the square of the strain associated with the misfit between cluster and host lattice, depends on their elastic properties, and is a complex function of the cluster shape (Eshelby, 1957). Assuming isotropic elasticity and incompressible clusters, Nabarro (1940) derived an expression for ΔG_E where the shape of the cluster can be described by an ellipsoid of revolution with the semi-axes a, a and c, separated from the host lattice by an incoherent interface. According to Nabarro (1940)

$$\Delta G_E = 6S\bar{v}e^2F\left(\frac{c}{a}\right) \tag{11}$$

where S is the shear modulus, e is the misfit strain, and F is a shape-dependent function of a and c. As can be seen from equation 11, ΔG_E is minimized if F approaches 0. In such a case, the shape of the cluster corresponds to that of a thin disc for which $c << a$.

Since both ΔG_E and the interfacial energy term depend on cluster shape, it may be assumed that the geometry of a cluster may be variable reflecting the minimization of ΔG^*. Lee *et al.* (1977) incorporated ΔG_E into the calculation of ΔG^* associated with the formation of clusters of varying shape that follow the geometric constraints of ellipsoids of revolution. According to Lee *et al.* (1977), ΔG_n may be expressed as

$$\Delta G_n = \frac{4\pi a^3}{3\bar{v}}\beta(\Delta G_V + \Delta G_E) + [2 + g(\beta)]\pi a^2\sigma \tag{12}$$

where β is the aspect ratio of the cluster, c/a, and $g(\beta)$ is given by

$$g(\beta) = \begin{cases} \frac{2\beta^2}{\sqrt{1-\beta^2}}\tanh^{-1}\left(\sqrt{1-\beta^2}\right) & \text{for } \beta<1 \\ 2 & \text{for } \beta=1 \\ \frac{2\beta}{\sqrt{1-\beta^{-2}}}\sin^{-1}\left(\sqrt{1-\beta^2}\right) & \text{for } \beta>1 \end{cases} \tag{13}$$

Differentiation of equation 12 with respect to a results in an expression for the critical radius that accounts for the influence of cluster shape on ΔG^*, and can be written as

$$a^* = \frac{-\bar{v}\sigma[2 + g(\beta)]}{2\beta(\Delta G_V + \Delta G_E)} \tag{14}$$

Substituting equation 14 into equation 12, one obtains:

$$\Delta G^*(\beta) = \frac{\pi\bar{v}^2\sigma^3[2 + g(\beta)]^3}{12\beta^2(\Delta G_V + \Delta G_E)^2} \tag{15}$$

Normalization of $\Delta G^*(\beta)$ with respect to the critical energy barrier for a spherical cluster shape in the absence of strain energy (ΔG^* in equation 5) results in

$$\frac{\Delta G^*(\beta)}{\Delta G^*} = \frac{[2 + g(\beta)]^3}{[8\beta(1 + \Delta G_E/\Delta G_V)]^2} \tag{16}$$

Figure 5 shows the variation of the normalized energy barrier, $\Delta G^*(\beta)/\Delta G^*$, with β for different ratios of $\Delta G_E/\Delta G_V$ for coherent nucleation (Lee *et al.*, 1977). In general, the normalized energy barrier rises with an increase of ΔG_E and a decrease of β. If ΔG_E contributes less than ~85% to the total bulk energy of cluster formation, a spherical cluster geometry ($\beta = 1$) results in a reduced energy barrier compared to cluster geometries with $\beta < 1$. It is only for higher relative contributions of ΔG_E that the energy barrier is minimized if the cluster geometry approaches the shape of an oblate spheroid. In those cases, the barrier is minimized if the cluster shape is that of a thin disk with β ranging between 0.2 and 0.3. In other words, if $|\Delta G_V|$ is large compared to ΔG_E, a spherical cluster shape may be a reasonable approximation of nucleus geometry provided that σ is isotropic.

1.1.3. Interfacial area

Critical cluster formation in the uniform region of the bulk matrix is referred to as homogenous nucleation. Heterogeneous nucleation refers to critical cluster formation in contact with a surface where interactions between cluster and surface reduce the energy barrier for nucleation. Heterogeneous nucleation commonly occurs at special sites such as foreign particles, crystal defects or grain boundaries. At these sites nucleation is catalysed because the interfacial energy and, hence, ΔG^*, are reduced.

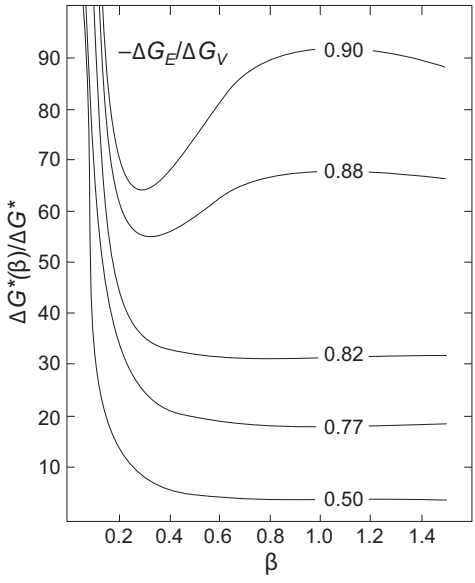

Figure 5. The normalized energy barrier, $\Delta G^*(\beta)/\Delta G^*$, as a function of β for different ratios of $\Delta G_E/\Delta G_V$ for isotropic coherent nucleation (after Lee *et al.*, 1977).

In the case of cluster formation on a flat surface in the absence of ΔG_E and considering isotropic interfacial energies, the cluster has the shape of a spherical cap the size of which is determined by the contact angle ϕ between the cluster and the reacting system (Fig. 6a). In this case, the critical energy barrier is reduced as a function of ϕ and is given by (Christian, 1975)

$$\Delta G^*_{\text{flat}} = f(\phi)\Delta G^* \tag{17}$$

where

$$f(\phi) = \tfrac{1}{4}(2 - 3\cos\phi + \cos^3\phi) \tag{18}$$

and

$$\cos\phi = (\sigma^{S\alpha} - \sigma^{S\beta})/\ \sigma^{\alpha\beta} \tag{19}$$

with

$$0 \leqslant \phi \leqslant 180^{\circ} \tag{20}$$

so that

$$\Delta G^*_{\text{flat}} = \frac{4\pi\bar{v}^2(\sigma^{\alpha\beta})^3(2 - 3\cos\phi + \cos^3\phi)}{3(\Delta G_V)^2} \tag{21}$$

If $\phi = 90^{\circ}$, the energy barrier to nucleation on the flat surface, ΔG^*_{flat}, is half of that required for homogenous nucleation, ΔG^*. For larger ϕ, ΔG^*_{flat} increases until it is equal to ΔG^* at $\phi = 180^{\circ}$. As ϕ approaches 0, ΔG^* decreases until it disappears at $\phi = 0$. This phenomenon is referred to as wetting of the surface or grain boundary.

Equation 21 may be a reasonable approximation for nucleation of a liquid from a gas at a flat surface, or precipitation on a mineral surface in contact with an aqueous solution. However, nucleation in most geological materials probably occurs on heterogeneities such as grain boundaries, grain edges or corners. For nucleation at a grain boundary the interfacial area of the cluster will be twice that of the $\alpha-\beta$ interface of the spherical cap (Fig. 6b) so that

$$\Delta G^*_{gb} = 2f(\phi)\Delta G^* = \frac{8\pi\bar{v}^2(\sigma^{\alpha\beta})^3(2 - 3\cos\phi + \cos^3\phi)}{3(\Delta G_V)^2} \tag{22}$$

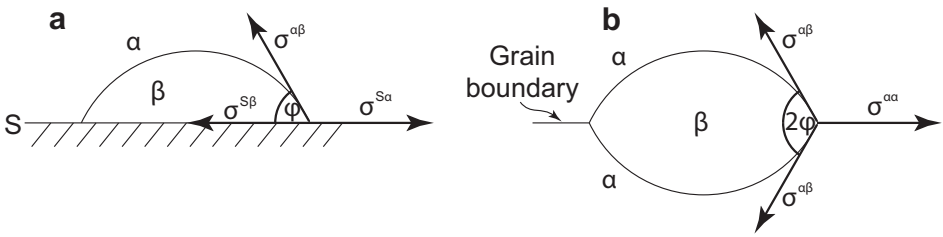

Figure 6. Geometry of (a) a cluster of phase β shaped as a spherical cup on a flat surface, surrounded by phase α, and (b) a lens-shaped cluster of phase β on a grain boundary in phase α.

Expressions similar to equations 21 and 22 can be derived for nucleation at grain edges or corners using their geometric relations for volume and interfacial area. According to Cahn (1956), the energy barrier decreases with a decrease in the dimensionality of the nucleation site. In other words, the barrier for nucleation along grain edges (1D) is less than that for nucleation along grain boundaries or cracks (2D) but larger than the energy barrier associated with nucleation at grain corners (0D). However, both the energy barrier to nucleation and the availability of the respective nucleation site in the reaction system dictate the rate of nucleation and how it changes in the course of the discontinuous phase transformation.

1.1.4. Nucleation at dislocations

In addition to grain boundaries, grain edges or corners, dislocations in host crystals are favourable sites for nucleation. However, their catalytic effect is fundamentally different from that exerted by the surfaces of grain boundaries or edges because the contact area between a dislocation and a cluster is too small to effectively reduce the interfacial area of a cluster. Similar to ΔG_V, the elastic strain energy of a dislocation released during nucleation is negative and may counteract the elastic misfit strain energy, ΔG_E, reducing the energy barrier to nucleation. The common migration of dislocations into sub-grain or small-angle grain boundaries indicates that nucleation at dislocations may not only take place in isolated areas in the interior of reacting crystals but that it may be a rather common type of nucleation, particularly during synkinematic metamorphic discontinuous phase transformations.

Cahn (1957) developed a formalism to treat nucleation at dislocations for the case that the interphase structure between cluster and reacting system is incoherent. According to Cahn (1957), the Gibbs energy per unit length of a cylindrical cluster forming on a dislocation considering an isotropic interfacial energy can be written as

$$\Delta G_D(r) = \frac{\pi r^2}{\bar{v}} \Delta G_V + 2\pi r\sigma - A \ln r \tag{23}$$

where the first term is the (negative) bulk contribution, r is the radial distance of the cylinder surface from the dislocation line, and $A\ln r$ reflects the elastic strain energy associated with the dislocation. For edge dislocations, A is given by

$$A_{\text{edge}} = \frac{Sb^2}{4\pi(1-\nu)}$$

and for screw dislocations

$$A_{\text{screw}} = \frac{Sb^2}{4\pi}$$

where b is the length of the Burgers vector and ν is Poisson's ratio. Because ν is ~0.3 for many solids, the difference in $\Delta G_D(r)$ between clusters at edge and screw dislocations may be ignored.

From equation 23 it follows that $\Delta G_D(r)$ develops a minimum at

$$r_0 = \frac{\bar{\nu}\sigma}{2\Delta G_V}(1 - \sqrt{1-\alpha}) \tag{24}$$

and a maximum at

$$r^* = \frac{\bar{\nu}\sigma}{2\Delta G_V}(1 + \sqrt{1-\alpha}) \tag{25}$$

where $\alpha = 2A\Delta G_V/\pi\bar{\nu}\sigma^2 < 1$ (Fig. 7a). r_0 corresponds to the radius of a metastable cylindrical cluster and is smaller than r^*, the radius of the critical cylindrical cluster that forms along the dislocation line. Beyond r^*, addition of molecules to the cluster surface will reduce the Gibbs energy of the system. Note that expressions (24) and (25) are based on the assumption that the length of the cluster corresponds to that of the dislocation line. A more realistic relationship is derived by Cahn (1957) using variational calculus methods in order to identify the cluster shape that reduces $\Delta G_D(r)^*$ the most. The resulting values for $\Delta G_D(r)^*$ are normalized with respect to the energy barrier to homogeneous nucleation, $\Delta G_H(r)^*$, and plotted against α in Fig. 7b. As can be seen, $\Delta G_D(r)^*/\Delta G_H(r)^*$ decreases drastically as α approaches unity. For $\alpha > 1$, the bulk energy term and the energy associated with the strain field around the dislocation balance the surface energy for all cluster sizes so that $\Delta G_D(r)$ does not contain extrema (Fig. 7a). In this case nucleation is effectively barrier-free and the discontinuous phase transformation depends entirely on the energetics and kinetics of crystal growth.

1.2. Rate of nucleation

In CNT, expressions for the rate of nucleation link the thermodynamics associated with the energy barrier to the kinetics of molecular attachment and detachment processes at the cluster/matrix interface. CNT predicts that once ΔG_V is negative, a finite number of

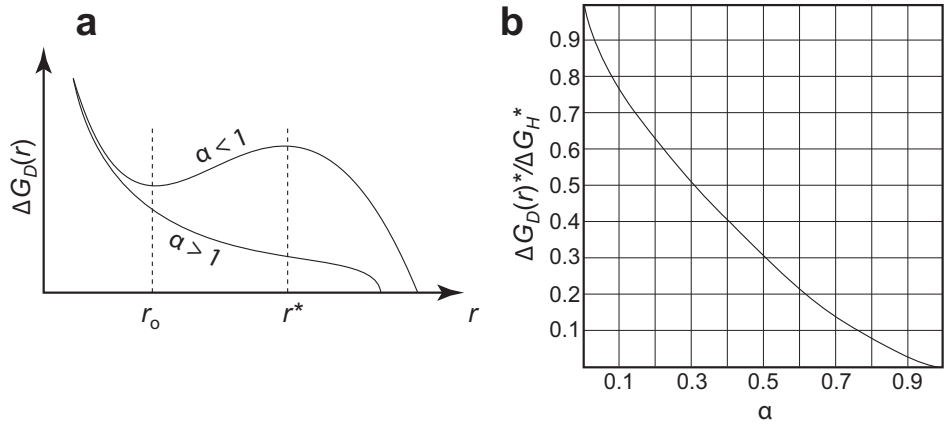

Figure. 7. (a) $\Delta G_D(r)$ *vs*. r of a cylindrical cluster surrounding a dislocation line. (b) $\Delta G_D(r)^*/\Delta G_H(r)^*$ *vs*. α for nucleation on a dislocation. After Cahn (1957).

clusters of various sizes is present, and that smaller ones are more abundant than larger ones (*e.g.* Christian, 1975; Kelton, 2006). Clusters of n molecules, E_n, are assumed to shrink or grow by loss or addition of a single molecule, E_1, through a series of bimolecular reactions

$$\begin{aligned} E_{n-1} + E_1 &\underset{k_n^-}{\overset{k_{n-1}^+}{\rightleftharpoons}} E_n \\ E_{n-1} + E_1 &\underset{k_{n+1}^-}{\overset{k_n^+}{\rightleftharpoons}} E_{n+1} \end{aligned} \tag{26}$$

where k_n^+ is the rate with which a molecule is attached to the surface of a cluster of size n and k_n^- is the rate of detachment of molecules from E_n. Impingement of clusters are assumed to be rare compared to the bimolecular reactions and are, therefore, not considered.

Based on reaction rate theory (Turnbull and Fisher, 1949) molecular attachment and detachment rates may be approximated by

$$\begin{aligned} k_n^+ &= O_n \gamma \exp\left(\tfrac{-\delta g_n}{2k_B T}\right) \\ k_{n+1}^- &= O_n \gamma \exp\left(\tfrac{+\delta g_n}{2k_B T}\right) \end{aligned} \tag{27}$$

where O_n is a geometrical factor reflecting the number of molecules that can be attached to the surface of a cluster composed of n molecules, $\delta g_n = \Delta G_{n+1} - \Delta G_n$ and γ is the molecular jump rate into and out of the cluster surface

$$\gamma = \frac{6D}{\lambda^2}$$

with the jump distance, $\lambda = \bar{v}^{1/3}$, and D, the molecular mobility at the interface. For spherical clusters, $O_n \approx 4n^{2/3}$ (Kelton *et al.*, 1983).

The cluster size frequency distribution $N_n(t)$ for homogenous nucleation can be derived by solving a modified system of Becker-Döring equations (Becker and Döring, 1935; Kelton, 1991)

$$\begin{aligned} \tfrac{\mathrm{dN_1}}{\mathrm{dt}} &= -\sum_{n=1}^{v-1} k_n^+ N_n + \sum_{n=2}^{v} (k_n^+ + k_n^-) N_n - \sum_{n=3}^{v+1} k_n^- N_n \\ \tfrac{\mathrm{dN_n}}{\mathrm{dt}} &= k_{n-1}^+ N_{n-1} - (k_n^- + k_n^+) N_n + k_{n+1}^- N_{n+1} \quad \text{for} \quad 1 < n < v \end{aligned} \tag{28}$$

where $v + 1$ is the upper limit of the range of cluster sizes that is considered. The numerical value of v depends on ΔG^* and is chosen to represent a cluster size that is bigger than the upper root of the $\Delta G(n)$ function (see Fig. 1). Following Kelton *et al.* (1983), $N_{n \geqslant v}(t)$ may be assumed to be zero to ensure that there is no backward flux of molecules from stable clusters. $N_1(t)$ is assumed to be the number of particles with single molecules which may decrease with time due to the formation of stable clusters, in particular in condensed geological materials. The modified system of Becker-Döring equations 28 accounts for the decrease in $N_1(t)$. It represents a numerically

stiff set of ordinary differential equations with the initial conditions (Gaidies *et al.*, 2011)

$$N_n(0) = \begin{bmatrix} N_1(0) \\ N_2(0) \\ \vdots \\ N_v(0) \end{bmatrix} = \begin{bmatrix} N^{\mathrm{eq}} \exp\left[\frac{-\Delta G_V}{k_B T}\right] \\ 0 \\ \vdots \\ 0 \end{bmatrix} \tag{29}$$

where N^{eq} is the number of molecules predicted to form at given *P-T-X* conditions during thermodynamic equilibrium. The nucleation rate can then be calculated as the flux of clusters past the critical cluster size and is given by

$$I^* = k^{+}_{n^*} N_{n^*} - k^{-}_{n^*+1} N_{n^*+1} \tag{30}$$

where N_{n^*} is the number of critical clusters.

The form of the heterogeneous nucleation rate equation is identical to that for homogenous nucleation (equations 28 to 30). However, for heterogeneous nucleation, and assuming that nucleation barriers are similar irrespective of the type of nucleation site, $N_1(t)$ does not correspond to the number of available monomers but reflects the number density of nucleation sites instead. Because the number of nucleation sites during heterogeneous nucleation is significantly smaller than the number of unclustered molecules, heterogeneous nucleation rates may be relatively low irrespective of the reduced energy barriers. In other words, the rate of heterogeneous nucleation depends on the number of available nucleation sites and their respective energy barriers and, hence, reflects the changes to the microstructure of the reacting system, such as grain-size reductions or changes to the dislocation density, that may evolve during crystallization. Considering that energy barriers in geological materials reflect a range of nucleation sites, and, hence, vary across the reacting system, different nucleation mechanisms may operate simultaneously at different locations in the system with the fastest mechanism dominating the overall nucleation rate.

It is important to note that, in addition to changes in ΔG^* and D, variations in the nucleation site density during crystallization result in changes to the overall nucleation rate. Therefore, a formalism similar to equation 28 may be best suited to numerically model time-dependent cluster-formation rates during heterogeneous nucleation in geological materials. This formalism also allows us to predict whether a steady-state nucleation rate may be established during the evolution of the cluster-size distribution.

Given that N_1 during homogenous nucleation in dilute systems is significantly larger than the number of critical clusters that form during the phase transformation, a steady-state nucleation rate may be approached in such a system. In this case, the steady-state nucleation rate, I^S, can be approximated by

$$I^S = O_{n^*} \gamma \exp\left(\frac{-\Delta G^*}{k_{\mathrm{B}} T}\right) N_1 Z$$

where Z is the dimensionless Zeldovich factor (Kelton, 2006)

$$Z = \sqrt{\frac{|\Delta G^*|}{3\pi k_B T n^*}}$$

which ranges commonly between 0.01 and 0.1. Z may be interpreted to correct for the backward flux of molecules associated with the decay of stable clusters.

Steady-state nucleation in condensed systems, such as during solid-state phase transformations associated with metamorphism, may be rather unlikely given the relatively small number of available nucleation sites. In fact, the number of energetically preferable nucleation sites may decrease significantly and approach the amount of critical clusters as metamorphic crystallization proceeds resulting in a reduction of the nucleation rate.

2. Coupled-flux analysis

Because CNT is an inherently interface-limited model, it cannot be applied to study nucleation in partitioning systems in which long-range diffusion across the reacting system is comparable to or slower than the molecular mobility at the cluster/matrix interface. If the capillarity approximation of CNT holds and the bulk term of the Gibbs energy of cluster formation can be separated from the interfacial term, the coupling of the flux across the interface with long-range diffusion may be simulated. Originally introduced by Russell (1968) and expanded by Kelton (2000), the coupled-flux approach considers a transitional domain that separates the cluster from the matrix (Fig. 8). At the domain/cluster interface a formalism similar to CNT is used where the energy barrier to homogenous nucleation is linked to the rates of molecular attachment and detachment processes. However, the bimolecular reaction rates applied in the coupled-flux analysis also consider the number of molecules available in the transitional domain, ρ, and the relative rates of the exchange of molecules between domain and cluster and between domain and matrix.

The exchange rates between transitional domain and matrix may be written as

$$\begin{aligned} \alpha(n, \rho - 1) &= \xi\rho \frac{D_m}{\lambda^2} \left(\frac{\rho_n^m - \rho + 1}{\rho} \right)^{1/2} \left(\frac{N_0}{N_S - N_0} \right)^{1/2} \\ \beta(n, \rho) &= \xi\rho \frac{D_m}{\lambda^2} \left(\frac{\rho_n^m - \rho + 1}{\rho} \right)^{-1/2} \left(\frac{N_0}{N_S - N_0} \right)^{-1/2} \end{aligned} \tag{31}$$

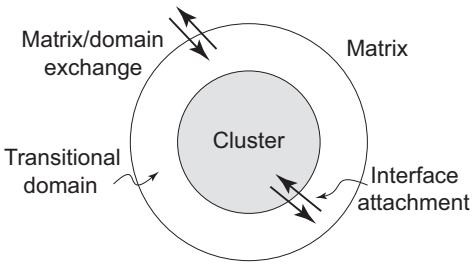

Figure 8. Schematic illustration of the coupled-flux model. After Russell (1968) and Kelton (2000).

where $\alpha(n,\rho-1)$ is the rate with which a molecule diffuses into the domain around a cluster of size n, and $\beta(n,\rho)$ is the rate with which it diffuses out of that domain into the matrix. D_m is the diffusion coefficient in the matrix, ρ_n^m is the maximum number of molecule sites available in the transitional domain surrounding a cluster of size n, and N_0 is the number of molecules distributed among N_S sites in the matrix per unit volume. ξ is a normalization constant. For a spherical cluster geometry, ρ_n^m increases approximately with cluster size as $4n^{2/3}$.

Similar to equation 27 but also accounting for the availability of molecules in the domain surrounding the cluster, the attachment and detachment rates at the cluster/domain interface can be approximated by

$$\begin{aligned} k_{n,\rho}^{+} &= \rho\gamma \exp\left(\frac{-\delta g_n}{2k_B T}\right) G(n,\rho) \\ k_{n+1,\rho-1}^{-} &= \rho\gamma \exp\left(\frac{+\delta g_n}{2k_B T}\right) \frac{1}{G(n,\rho)} \end{aligned} \tag{32}$$

where the correction factor $G(n,\rho)$ considers the changes in entropy in the transitional domain and matrix caused by the attachment of a molecule to the cluster surface

$$G(n,\rho) = \frac{1}{\sqrt{\frac{\alpha_n \rho_n^m!(\rho_{n+1}^m-\rho+1)!}{\alpha_{n+1}\rho_{n+1}^m!\rho(\rho_{n+1}^m-\rho)!}\left(\frac{N_0}{N_S-N_0}\right)}}$$

For a fast exchange between matrix and domain relative to γ, $G(n,\rho) = 1$ and $\rho = \rho_n^m$. In this case, equation 32 is identical to equation 27 of CNT, and the nucleation rate is controlled by the rate of the interface processes.

Note that ΔG_V is considered independent of the rates of interface processes and matrix diffusion. For the calculation of ΔG_V it is assumed that there are no chemical potential gradients across the matrix so that the cluster composition for all sizes is fixed and defined by the maximum Gibbs energy dissipation after some departure from equilibrium. The coupled differential equations required to quantify the cluster size frequency distribution $N_{n,\rho}(t)$ can then be written as

$$\frac{dN_{n,\rho}}{dt} = I_{n-1} - I_n + J_{\rho-1} - J_\rho \tag{33}$$

where

$$\begin{aligned} I_{n-1} &= N_{n-1,\rho+1} - N_{n,\rho}k_{n,\rho}^{-} \\ I_n &= N_{n,\rho}k_{n,\rho}^{+} - N_{n+1,\rho-1}k_{n+1,\rho-1}^{-} \\ J_{\rho-1} &= N_{n,\rho-1}\alpha_{n,\rho-1} - N_{n,\rho}\beta_{n,\rho} \\ J_\rho &= N_{n,\rho}\alpha_{n,\rho} - N_{n,\rho+1}\beta_{n,\rho+1} \end{aligned}$$

Solution of equation 33 for the case of slow matrix diffusion relative to the chemical mobility at the cluster surface indicates that the transitional domains around subcritical clusters become enriched during the discontinuous phase transformation while the

domains surrounding supercritical clusters become deplete with respect to the number of molecules available for cluster formation compared to the average matrix composition. In addition, nucleation rates become smaller than calculated from CNT, and the time required to establish a steady state during homogenous nucleation increases as long-range diffusion becomes more important.

The spatial extent of the depletion zone around a supercritical cluster that develops during diffusion-controlled nucleation cannot be predicted with the coupled-flux model. However, the extent of depletion must reflect the matrix diffusivity and the increase in volume of the growing cluster. The addition of molecules to the cluster may reduce the chemical potential of the diffusing component in the vicinity of the cluster depending on the $G{-}x$ relationship of the matrix. If there are local sinks in the chemical potential around the supercritical cluster, the chemical driving force for nucleation available in the depletion zone would be lower than in the matrix, and the energy barrier to nucleation in this zone may not be overcome. Nucleation in the depletion zone may only be possible if there are reductions to the energy barrier to nucleation across this zone. Possible scenarios that may explain nucleation within the depletion zone include the drastic increase in ΔG_V as a response to changes in P, T, X during crystallization, a decrease in ΔG_E, or a decrease of the interfacial area and an increase in the number of nucleation sites caused by the reduction of grain size in the reacting system.

3. Nucleation in inhomogeneous systems

The separation of bulk and interface terms in the energetics of cluster formation is referred to as capillarity approximation and limits the applicability of CNT to discontinuous phase transformations close to equilibrium. In such a case, the reacting system and nucleating phase may be considered homogenous separated by a sharp, thin interface. However, nucleation at significant departure from equilibrium may result in critical sizes too small for the capillarity approximation to be valid. In this case, the interface may be diffuse and reactant and nucleus may be considered inhomogeneous instead. Non-classical gradient-energy continuum approaches to nucleation allow prediction of the properties of a critical cluster also at significant departure from equilibrium.

3.1. Gradient-energy continuum approach

If an initially homogeneous thermodynamically stable system is quenched into a two-phase field through a rapid variation of pressure or temperature, it may become unstable or metastable depending on its composition (Fig. 9a). In case the system is quenched into an unstable state, it tends toward equilibrium through the process of spinodal decomposition. The $G{-}x$ relationship of the unstable system is characterized by a curvature that is convex towards higher values of G so that $\partial^2 G/\partial x^2 < 0$ and infinitesimal fluctuations in x reduce G initiating the phase transformation (Fig. 9a). This type of phase transformation is referred to as *continuous* and is not associated with any energy barrier other than those required for chemical diffusion of components between the coexisting phases.

If the $G{-}x$ relationship within the two-phase region is characterized by a curvature that is concave towards higher values of G so that $\partial^2 G/\partial x^2 > 0$ (Fig. 9a), the system

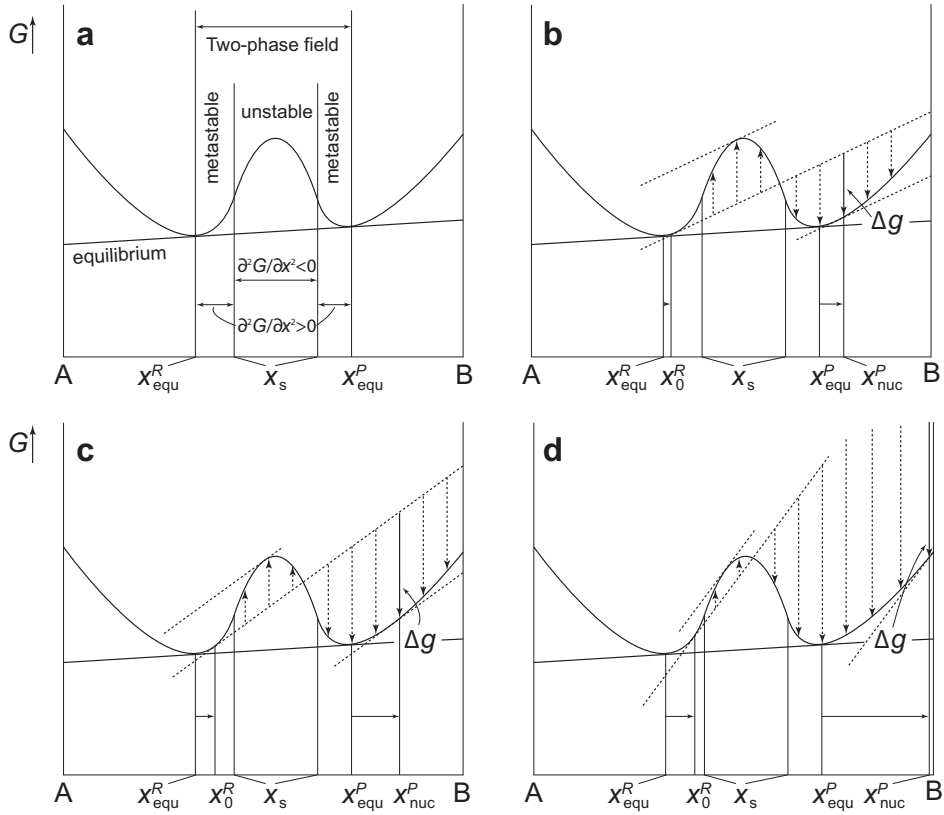

Figure 9. Schematic molar *G*-*x* diagrams showing the chemical driving force for nucleation, Δg, for different degrees of supersaturation. Nucleation takes place in the metastable region of the two-phase field.

experiences a metastable state and small fluctuations in x increase the Gibbs energy of the system. The extent of metastability is limited by the chemical spinodal ($\partial^2 G/\partial x^2 = 0$) and binodal ($x_s$ and x^R_{equ}, respectively, in Fig. 9). In order to re-establish equilibrium, large fluctuations in x are required to decrease the Gibbs energy. These fluctuations may be compared to critical clusters, and the energy barrier that has to be overcome for their formation may be referred to as the energy barrier to nucleation characteristic for *discontinuous* phase transformations. The energy barrier to nucleation is largest close to equilibrium ($x^R_0 \rightarrow x^R_{equ}$ in Fig. 9b) and decreases towards the spinodal ($x^R_0 \rightarrow x_s$ in Fig. 9d). The energy barrier to nucleation vanishes at the chemical spinodal.

The chemical driving force for nucleation in a system with double-well potential can be obtained through the parallel tangent method (Δg in Fig. 9b–d). It is the maximum difference in Gibbs energy between the critical cluster and the reacting system and increases with departure from equilibrium ($x^R_0 \rightarrow x_s$). Whereas the properties of reacting system and nucleus for phase transformations close to equilibrium do not vary

significantly with x, so that the phases may be approximated as homogeneous, relatively small variations in x influence significantly G of the reacting system and nucleus as the departure from equilibrium increases (Fig. 9).

The influence of chemical heterogeneity on the energetics of nucleation can be estimated using the gradient-energy approach of Cahn and Hilliard (1958)

$$G = \int_v \left[g(x) + \kappa_x (\nabla x)^2 \right] \mathrm{d}V \tag{34}$$

where $g(x)$ is the Gibbs energy of a homogeneous system at composition x, and κ_x is a positive materials constant referred to as the compositional gradient energy coefficient. κ_x corrects for the spatial chemical heterogeneity and is derived through a Taylor series expansion of g in powers of ∇x where the series is truncated after the quadratic term and the linear terms neglected due to symmetry requirements. Because x describes a field in an inhomogeneous system, G is a functional of the composition field integrated over the volume of the system.

According to Cahn and Hilliard (1959), the energy barrier to nucleation in an inhomogeneous system can be expressed as

$$\Delta G^* = \int_V \left[\Delta g(x) + \kappa_x (\nabla x)^2 \right] \mathrm{d}V \tag{35}$$

and, assuming a spherical nucleus geometry,

$$\Delta G^* = 4\pi \int_0^\infty \left[\Delta g(x) + \kappa_x \left(\frac{\mathrm{d}x}{\mathrm{d}r} \right)^2 \right] r^2 \mathrm{d}r \tag{36}$$

subject to the boundary conditions

$$\frac{\mathrm{d}x}{\mathrm{d}r} \to 0 \text{ as } r \to 0 \text{ and } r \to \infty$$

and

$$x \to x_0^R \text{ as } r \to \infty$$

where x_0^R is the composition of the reactant (Fig. 9). ΔG^* is a saddle point of the G functional and approaches the classical energy barrier to nucleation only for phase transformations close to equilibrium. In this case, interface curvature and thickness are minimized and the size of a critical cluster approaches infinity. However, with increasing departure from equilibrium, the critical energy barrier determined through the Cahn-Hilliard model decreases more than that of CNT and becomes zero at the chemical spinodal. In contrast, CNT predicts that the energy barrier vanishes only for an infinitely large degree of departure from equilibrium (*e.g.* equation 5). Another fundamental difference between the predictions of CNT and the Cahn-Hilliard gradient energy approach concerns the size of the critical cluster. Whereas CNT predicts an exceedingly small critical

size far from equilibrium (*e.g.* equation 4), the non-classical gradient energy approach predicts that the size of the critical fluctuation diverges at the spinodal after it experiences a minimum at intermediate degrees of supersaturation (Fig. 10).

In the Cahn-Hilliard gradient energy model, the energy barrier to nucleation is a function of the properties of the "hump" in the $G-x$ function of the system (Fig. 9), and the gradient energy term. The energy barrier increases and the interface thins and gets sharper as the size of the "hump" increases. The gradient energy term increases the thickness of the interface and smoothens the compositional gradient across it. In contrast to CNT where interfaces are characterized by sharp structural differences between the reacting system and nucleus, interfaces in the Cahn-Hilliard gradient-energy model are defined as locations with significant compositional gradients. The excess energy associated with these compositional gradients constitutes the interfacial energy, and there are no structural differences between reacting system and nucleus.

If a phase transformation is isochemical and associated only with a transition in structure then the Cahn-Hilliard approach cannot be used to quantify the energy barrier to nucleation and the size of a nucleus. Instead, the Allen-Cahn approach (Allen and Cahn, 1979) may be applied which allows us to model continuous order-disorder phase transformations. The Gibbs energy may then be written

$$G = \int_V \left[g(\eta) + \kappa_\eta (\nabla \eta)^2 \right] \mathrm{d}V \tag{37}$$

where $g(n)$ is the Gibbs energy of the homogeneous system, η is a long-range order parameter and κ_η is the gradient energy coefficient for that order parameter.

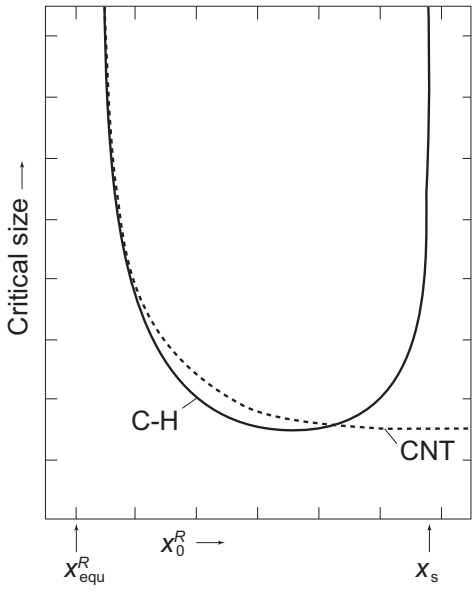

Figure 10. Schematic relationship between the size of a critical cluster and the departure from equilibrium according to the classical nucleation theory (CNT) and the Cahn-Hilliard gradient energy approach (C-H). Modified after Cahn and Hilliard (1959).

Poduri and Chen (1996) developed a model that describes phase transformations involving both compositional and structural changes combining the Cahn-Hilliard and Allen-Cahn approaches. According to Poduri and Chen (1996), the increase in Gibbs energy arising from the formation of a spherical nucleus is given by

$$\Delta G^{*} = 4\pi \int \left[\Delta g(\eta, x) + \kappa_{\eta} \left(\frac{\mathrm{d}\eta}{\mathrm{d}r} \right)^{2} + \kappa_{x} \left(\frac{\mathrm{d}x}{\mathrm{d}r} \right)^{2} \right] r^{2} \mathrm{d}r \tag{38}$$

Similar to the Cahn-Hilliard approach, the non-classical critical cluster size determined by Poduri and Chen (1996) diverges at the spinodal. However, according to Binder (1991), the divergence of the critical size is an artefact of the gradient energy approach if thermal fluctuations are ignored. It has been suggested (Poduri and Chen, 1996) that the incorporation of a thermal noise term in the calculation of the nucleation energetics, as initially proposed by Cook (1970), does result in finite critical sizes also for nucleation close to the spinodal.

The Cahn-Hilliard gradient energy approach is similar to a model initially developed by van der Waals (1893). More advanced models of nucleation derived by Oxtoby and Evans (1988), Bagdassarian and Oxtoby (1994) and Granasy *et al.* (2002) are based on the pioneering work of van der Waals and Cahn-Hilliard and are similar in that the gradient energy terms act as a penalty for sharp compositional or structural gradients allowing for the modelling of interfacial tension between reacting system and nucleus. The treatment of Bagdassarian and Oxtoby (1994), however, predicts a decrease in both, ΔG^{*} and r^{*} with departure from equilibrium, with ΔG^{*} vanishing and r^{*} taking on a finite size at the spinodal. In the work by Bagdassarian and Oxtoby (1994), a thermal noise term, as suggested by Binder (1991), was not required to predict more realistic nucleus sizes at the spinodal. Instead, the homogeneous Gibbs energy functional was modelled with two parabolas, each centred with their minimum on the reacting and nucleating phase, respectively, and intersecting at a Gibbs energy related to the driving force for nucleation (Bagdassarian and Oxtoby, 1994). According to this work, r^{*} increases away from the spinodal and is identical to the classical critical radius close to equilibrium if the curvatures of the two parabolas are the same. In case the Gibbs energy curvature of the parabola about the nucleus is greater than that about the reacting system, the predicted critical size close to equilibrium is greater than the classical one. The Bagdassarian and Oxtoby (1994) model of intersecting Gibbs energy parabolas may be a valuable approach to study the energetics of nucleation in geological materials if the curvatures of the parabolas are fit to the realistic Gibbs energy profiles of the geological phases. The phase field method may then be used to predict the dynamics of nucleation and microstructure evolution.

3.2. Nucleation simulations with the phase field method

The gradient energy approach allows us to model the microstructural evolution of a system during a discontinuous phase transformation if linked to rate expressions for nucleation and growth. Such evolution models constitute the phase field method (*e.g.*

Chen, 2002) which requires the description of the Gibbs energy density as a function of field variables, commonly referred to as order parameters, such as system composition and structure. The two most common approaches to the dynamics of nucleation in a phase field model are the introduction of a random noise term to simulate thermal fluctuations (*e.g.* Wang *et al.*, 1995), and the explicit nucleation method (*e.g.* Simmons *et al.*, 2000). In any case, the phase field method is a computational tool applied to the study of the dynamics of nucleation where the microstructure evolution of the model system is driven by an overall reduction of Gibbs energy. Because it considers the influence of spatial variations in order parameters on the Gibbs energy of the system, the phase field method allows us to study potential interactions between neighbouring nuclei such as the competition for nutrients during diffusion-controlled cluster formation or the coalescence of nuclei. It is important to note that the capillarity approximation and the interface-controlled kinetics inherent in CNT do not allow for a similar treatment limiting it to a 0-dimensional theory.

The random noise phase field method (*e.g.* Wang *et al.*, 1995) adds Langevin random fluctuation terms (Landau and Lifshitz, 1969) both to the stochastic Cahn-Hilliard time evolution equation (Cahn and Hilliard, 1958) and to the Allen-Cahn time evolution equation (Allen and Cahn, 1979) so that

$$\frac{\partial x}{\partial t} = M\left[\frac{\partial^2 g(\eta, x)}{\partial x^2}\nabla^2 - 2\kappa_x \nabla^4 x\right] + \xi$$

and

$$\frac{\partial \eta}{\partial t} = -L\left[\frac{\partial g(\eta, x)}{\partial \eta} - 2\kappa_\eta \nabla^2 \eta\right] + \xi$$

where t is time, M and L are the positive kinetic coefficients related to the diffusional mobility and the microscopic rearrangement kinetics, respectively, and ξ is the Langevin noise term satisfying the fluctuation-dissipation theorem (Landau and Lifshitz, 1969). $g(\eta,x)$ is usually approximated by a Landau expansion polynomial

$$g(\eta, x) = \frac{A_1}{2}(x - x_1)^2 + \frac{A_2}{2}(x - x_2)(\eta_1^2 + \eta_2^2) - \frac{A_3}{4}(\eta_1^4 + \eta_2^4) + \frac{A_4}{6}(\eta_1^2 + \eta_2^2)^3$$

where x_1, x_2, A_i ($i = 1,...4$) are positive constants and η_1 and η_2 are the long-range order parameters. x_1 and x_2 are close to the equilibrium compositions of the reactant and nucleus, and the A_i values define the shape of the Gibbs energy surface.

The random noise phase field method has been shown to allow appropriately for the simulation of homogeneous (Wang *et al.*, 1995) and heterogeneous (Castro, 2003) nucleation if the energy barrier to nucleation is relatively small. However, unphysically large random noise is required to simulate discontinuous phase transformations in systems with significant energy barriers to nucleation which results in unrealistic nucleation-rate predictions. In addition, the high spatial and temporal resolution of the simulations required by the Langevin noise terms is computationally prohibitive unless they are applied to very small model systems.

The explicit nucleation model (*e.g.* Simmons *et al.*, 2000; Jokisaari *et al.*, 2016) may be considered a valuable alternative to the random noise phase field method as it is computationally less expensive. It allows us to link the time evolution equations of the phase field method with the nucleation energetics and nucleus sizes derived either through CNT (*e.g.* Simmons *et al.*, 2000) or the gradient-energy approach (*e.g.* Heo *et al.*, 2010). The Langevin noise terms are not included in the explicit nucleation method. Instead, the nuclei are introduced explicitly to the system assuming that the time required for their formation is significantly shorter than the temporal resolution of the nucleation simulation, Δt. At random locations, r, nucleation probabilities, P, are calculated through

$$P(r,t) = 1 - \exp(-I^*\Delta t)$$

and compared to a uniform random number, R, which ranges between 0 and 1. In case $P > R$, a nucleus is placed at the respective location, and the local composition field is depleted accordingly to account for the conservation of the overall composition if the phase transformation is partitioning.

The time evolution equations of the phase field method are coupled partial differential equations that can be solved numerically in various ways, including finite differences and spectral methods, and the finite element method. These numerical approaches allow the simulation of nucleation even in complex geometries, such as those associated with dendrite formation (*e.g.* Granasy *et al.*, 2004a,b), and have been successfully used to study nucleation in multiphase systems (*e.g.* Steinbach *et al.*, 1996; Nishida *et al.*, 2014). The additional consideration of growth kinetics (see Gaidies *et al.* 2017, this volume) allows the analysis of the complete microstructure evolution of the system associated with the discontinuous phase transformation.

4. Summary and potential future research

Nucleation is a fundamental process during most phase transformations in geological materials. CNT may be used to characterize the energetics of the critical barrier and the rate of nucleation for reactions close to equilibrium provided that long-range diffusion is fast relative to attachment and detachment processes at the interface between nucleus and metastable reactant. Non-classical gradient energy approaches to nucleation, such as the Bagdassarian and Oxtoby (1994) model, may be valuable alternatives to CNT as they allow the consideration of the influence of chemical heterogeneities on nucleation kinetics. Such heterogeneities may form in the metastable matrix in the vicinity of a nucleus during diffusion-controlled nucleation, or across the nucleus/matrix interface during nucleation far from equilibrium where the nucleus is assumed to be so small that interface properties are rather diffuse. The most promising approach to study the spatial distribution and evolution of nuclei in multiphase systems, such as most geological materials, may be the phase field method. Application of this method to appropriate systems may result in a better understanding of nucleation in geological materials and its influence on micro-structure and rock-texture formation.

Acknowledgements

The author thanks R. Abart for numerous discussions and his editorial advice, and F. George for valuable comments on an earlier draft of this chapter. Detailed comments and suggestions by E. Petrishcheva significantly helped to improve the presentation of this chapter.

References

Allen, S.M. and Cahn, J.W. (1979) A microscopic theory for antiphase boundary motion and its application to antiphase domain coarsening. *Acta Metallurgica*, **27**, 1085–1095.

Bagdassarian, C.K. and Oxtoby, D.W. (1994) Crystal nucleation and growth from the undercooled liquid: A nonclassical piecewise parabolic free-energy model. *Journal of Chemical Physics*, **100**, 2139–2148.

Becker, R. and Döring, W. (1935) Kinetische Behandlung der Keimbildung in übersättigten Dämpfen. *Annalen der Physik*, **24**, 719–752.

Binder, K. (1991) Spinodal decomposition in materials science and technology. Pp. 405–471 in: *Phase Transformations in Materials* (P. Haasen, editor), **5**. Wiley-VCH Verlag GmbH, Weinheim, Germany.

Cahn, J.W. (1956) The kinetics of grain boundary nucleated reactions. *Acta Metallurgica*, **4**, 449–459.

Cahn, J.W. (1957) Nucleation on dislocations. *Acta Metallurgica*, **5**, 169–172.

Cahn, J.W. and Hilliard, J.E. (1958) Free energy of a nonuniform system. I. Interfacial free energy. *The Journal of Chemical Physics*, **28**, 258–267.

Cahn, J.W. and Hilliard, J.E. (1959) Free energy of a nonuniform system. III. Nucleation in a two-component incompressible fluid. *The Journal of Chemical Physics*, **31**, 688–699.

Castro, M. (2003) Phase-field approach to heterogeneous nucleation. *Physical Review B*, **67**, 035412.

Chen, L.Q. (2002) Phase-field models for microstructure evolution. *Annual Review of Materials Research*, **32**, 113–140.

Christian, J.W. (1975) *The Theory of Transformations in Metals and Alloys: Part 1 – Equilibrium and General Kinetic Theory*. Pergamon Press, Oxford, UK.

Cook, H.E. (1970) Brownian motion in spinodal decomposition. *Acta Metallurgica*, **18**, 297–306.

Eshelby, J.D. (1957) On the determination of the elastic field of an ellipsoidal inclusion, and related problems. *Proceedings of the Royal Society*, **A 241**, 376– 396.

Frenkel, J. (1946) *Kinetic Theory of Liquids*. Oxford University Press, Oxford, UK.

Gaidies, F., Pattison, D.R.M. and de Capitani, C. (2011) Toward a quantitative model of metamorphic nucleation and growth. *Contributions to Mineralogy and Petrology*, **162**, 975–993.

Gaidies, F., Milke, R., Heinrich, W. and Abart, R. (2017) Metamorphic mineral reactions: Porphyroblast, corona and symplectite growth. Pp. 469–540 in: *Mineral Reaction Kinetics: Microstructures, Textures and Chemical Compositions* (R. Abart and W. Heinrich, editors). EMU Notes in Mineralogy, **16**. European Mineralogical Union and Mineralogical Society of Great Britain & Ireland, London.

Gibbs, J.W. (1928) *The Collected Works. Vol. 1 Thermodynamics*. Longmans, Green & Co, New York.

Granasy, L., Pusztai, T. and James, P.F. (2002) Interfacial properties deduced from nucleation experiments: A Cahn-Hilliard analysis. *Journal of Chemical Physics*, **117**, 6157–6168.

Granasy, L., Pusztai, T., Börzsonyi, T., Warren, J.A. and Douglas, J.F. (2004a) A general mechanism of polycrystalline growth. *Nature Materials*, **3**, 645–650.

Granasy, L., Pusztai, T. and Warren, J.A. (2004b) Modelling polycrystalline solidification using phase field theory. *Journal of Physics: Condensed Matter*, **16**, R1205–R1235.

Heo, T.W., Zhang, L., Du, Q. and Chen, L.Q. (2010) Incorporating diffuse-interface nuclei in phase-field simulations. *Scripta Materialia*, **63**, 8–11.

Holland, T.J.B. and Powell, R. (1998) An internally consistent thermodynamic data set for phases of petrological interest. *Journal of Metamorphic Geology*, **16**, 309–343.

Jokisaari, A.M., Permann, C. and Thornton, K. (2016) A nucleation algorithm for the coupled conserved–nonconserved phase field model. *Computational Materials Science*, **112**, 128–138.

Kaischew, R. and Stranski, I.N. (1934) Concerning the mechanism of the equilibrium of small crystals. *Zeitschrift für Physikalische Chemie-Abteilung B- Chemie der Elementarprozesse Aufbau der Materie*, **26**, 312–316.

Kelton, K.F. (1991) Crystal nucleation in liquids and glasses. Pp. 75–178 In: *Solid State Physics* (H. Ehrenreich, and D. Turnbull, editors), **45**. Academic Press, London.

Kelton, K.F. (2000) Time-dependent nucleation in partitioning transformations. *Acta Materialia*, **48**, 1967–1980.

Kelton, K.F. (2006) Nucleation. Pp. 6388–6393 in: *Encyclopedia of Materials: Science and Technology* (K.H. Buschow, R.W. Cahn, M.C. Flemings, B. Ilschner, E.J. Kramer, S. Mahajan and P. Veyssiere, editors), **7**. Elsevier, Amsterdam.

Kelton, K.F., Greer, A.L. and Thompson, C.V. (1983) Transient nucleation in condensed systems. *Journal of Chemical Physics*, **79**, 6261–6276.

Landau, L.D. and Lifshitz, E.M. (1969) *Statistical Physics*, 2nd edition. Pergamon Press, New York.

Lee, J.K., Barnett, D.M. and Aaronson, H.I. (1977) The elastic strain energy of coherent ellipsoidal precipitates in anisotropic crystalline solids. *Metallurgical Transactions A*, **8A**, 963–970.

Nabarro, F.R.N. (1940) The influence of elastic strain on the shape of particles segregating in an alloy. *Proceedings of the Physical Society*, **52**, 90–104.

Nishida, Y., Aiga, F. and Itoh, S. (2014) Microstructural path analysis of polycrystalline solidification by using multi-phase-field method incorporating a nucleation model. *Journal of Crystal Growth*, **405**, 110–121.

Oxtoby, D.W. and Evans, R. (1988) Nonclassical nucleation theory for the gas-liquid transition. *Journal of Chemical Physics*, **89**, 7521–7530.

Poduri, R. and Chen, L.Q. (1996) Non-classical nucleation theory of ordered intermetallic precipitates – application to the Al-Li alloy. *Acta Materialia*, **44**, 4235–4259.

Russell, K.C. (1968) Linked flux analysis of nucleation in condensed phases. *Acta Metallurgica*, **16**, 761–769.

Simmons, J.P., Shen, C. and Wang, Y. (2000) Phase field modeling of simultaneous nucleation and growth by explicitly incorporating nucleation events. *Scripta Materialia*, **43**, 935–942.

Steinbach, I., Pezzolla, F., Nestler, B., Sesselberg, M., Prieler, R., Schmitz, G.J., Rezende, J. L.L. (1996) A phase field concept for multiphase systems. *Physica D*, **94**, 135–147.

Turnbull, D. and Fisher, J.C. (1949) Rates of nucleation in condensed systems. *Journal of Chemical Physics*, **17**, 71–73.

van der Waals, J.D. (1893) Thermodynamische Theorie der Kapillarität unter Voraussetzung stetiger Dichteänderung. *Zeitschrift für Physikalische Chemie*, **13**, 675–725.

Volmer, M. (1939) *Kinetik der Phasenbildung*. Steinkopf, Dresden, Germany.

Volmer, M. and Weber, A. (1926) Keimbildung in übersättigten Gebilden. *Zeitschrift für Physikalische Chemie*, **119**, 277–301.

Wang, Y., Wang, H.-Y., Chen, L.Q. and Khachaturyan, A.G. (1995) Microstructural development of coherent tetragonal precipitates in Magnesium-partially-stabilized zirconia: a computer simulation. *Journal of the American Ceramic Society*, **78**, 657–661.